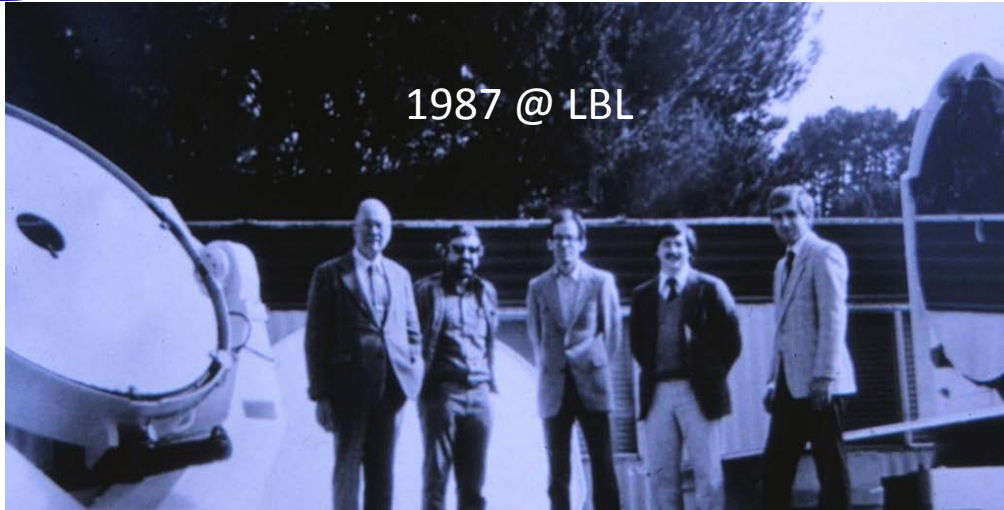




Infrared spatial interferometer (ISI)

High Spectral resolution, high angular resolution and new techniques

C. Townes, W. Fitelson, E. Sutton, W. Danchi, M. Bester



1987 @ LBL

K.S. Abdeli	R.L. Griffith	B. Mukergee	Manfred Bester
P. Barele	D.D.S. Hale*	B. Pope	B. Walp
M. Bester	S. Hoss	V. Ravi	J. Weiner*
A. Betz*	J. Hudson	K. Reichl	R.H. Weitzman
K. Blanchard	M. Johnson*	J. Remy	E.H. Wishnow
A.A. Chandler	K. Konevsky	C.S. Ryan	
J. Cobb	E.A. Lipman*	B. Saduolet	
J. Chu	S. Lockwood	J. Shapiro	
W.C. Danchi	B. Lopez	N. Short	
C.G. Degiacomi	W. Mallard	J. Storey	
M. Ellison	T. MacDonald	E.C. Sutton*	
R. Fulton	J. McMahon	K Tatebe*	
D. Finstad	H. Mistry	S. Tevousian	
W. Fitelson	D. Michaud	P.G. Tuthill	
L.J. Greenhill	J.D. Monnier*	V. Toy	



2008 @ Mt. Wilson

Cristina Ryan

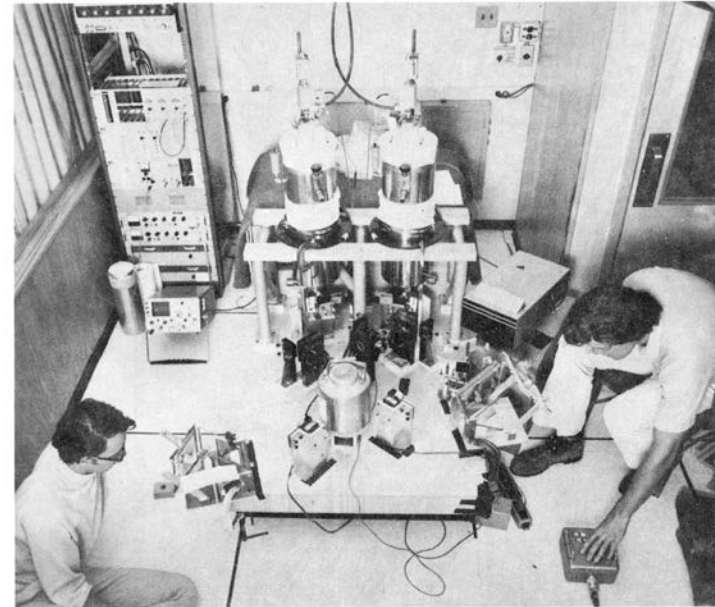
and many more...

Grad students get a *



Heterodyne det. demonstration at McMath-Pierce tele. Kitt Peak

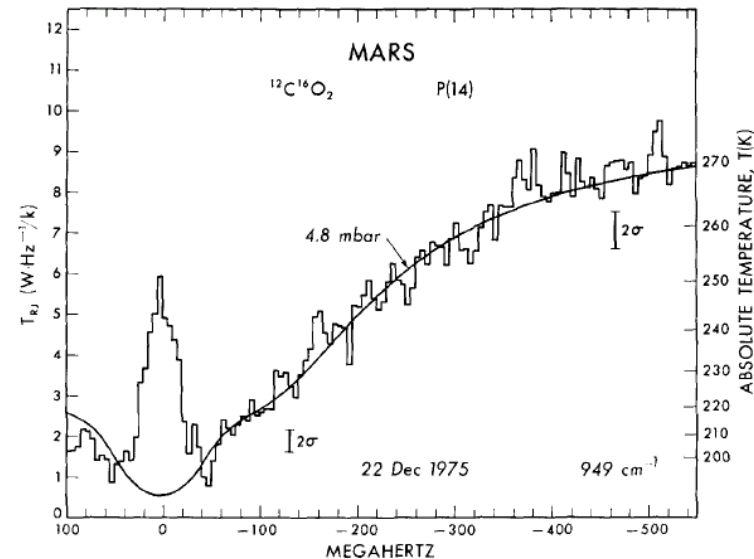
New techniques, High spectral resolution



10 μm interferometry using heterodyne detection.
 5.5 m baseline between auxiliary siderostats
 Johnson, Betz, Townes 1974
 Atmosphere shown to be stable enough for interference
 fringes from Mercury to be detected.

Also high resolution spectroscopy of Venus,
 Mars, and stellar environs.
 Right: Very sharp CO₂ line in Martian atm.
 later called “natural lasers on Mars”

Kostiuk et al. at GSFC, het. spect. on Subaru
 Ethane & winds on Titan using ¹⁴CO₂ LO lines





Infrared Spatial Interferometer



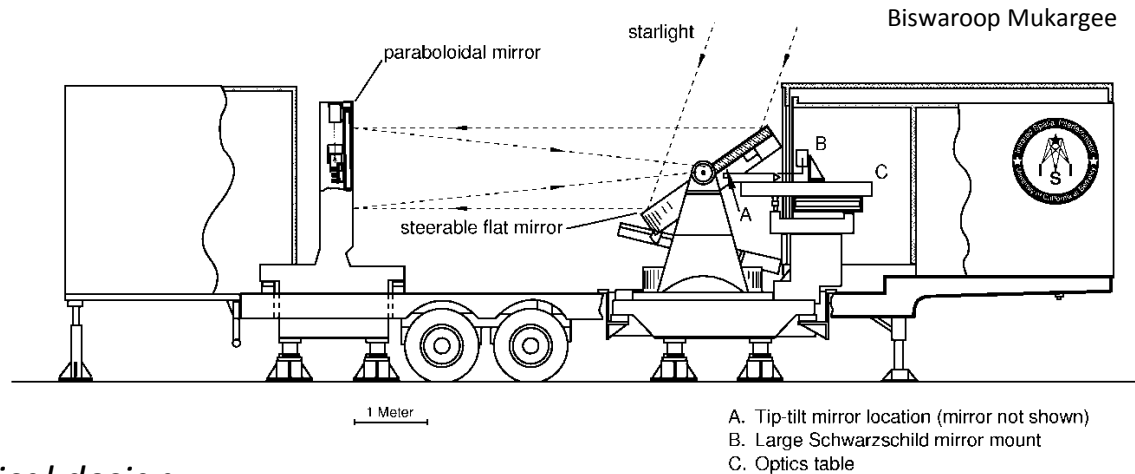
World's highest frequency radio telescope interferometer, operates at 27 THz ($11\ \mu\text{m}$). Heterodyne detection using $^{13}\text{C}^{16}\text{O}_2$ lasers as local oscillators. Geometric delays removed using RF delay lines.

Currently located at Mt. Wilson Observatory, a site noted for very stable seeing.



*Two telescopes in operation 1988
First fringes 1988
Third telescope 2003
Closure phase measured 2004*

Telescopes designed for transport as a standard semi-trailer



*Pfund optical design,
65" f/3.14 parabolic primary, 80" flat mirror*

Interferometry principle of operation: Definition of “Visibility”

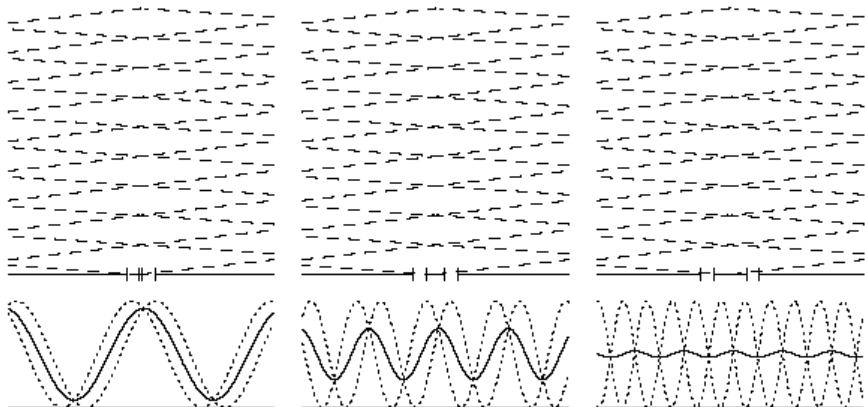
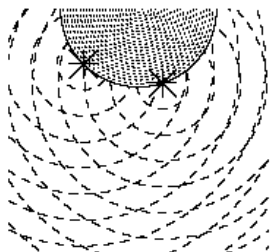
Mathematical description: Visibility is the complex 2D FFT of the 2D source intensity distribution (Van Cittert-Zernike theorem)

Phenomenological description: The envelope of fringes in a Young’s double slit experiment gives information on the source size

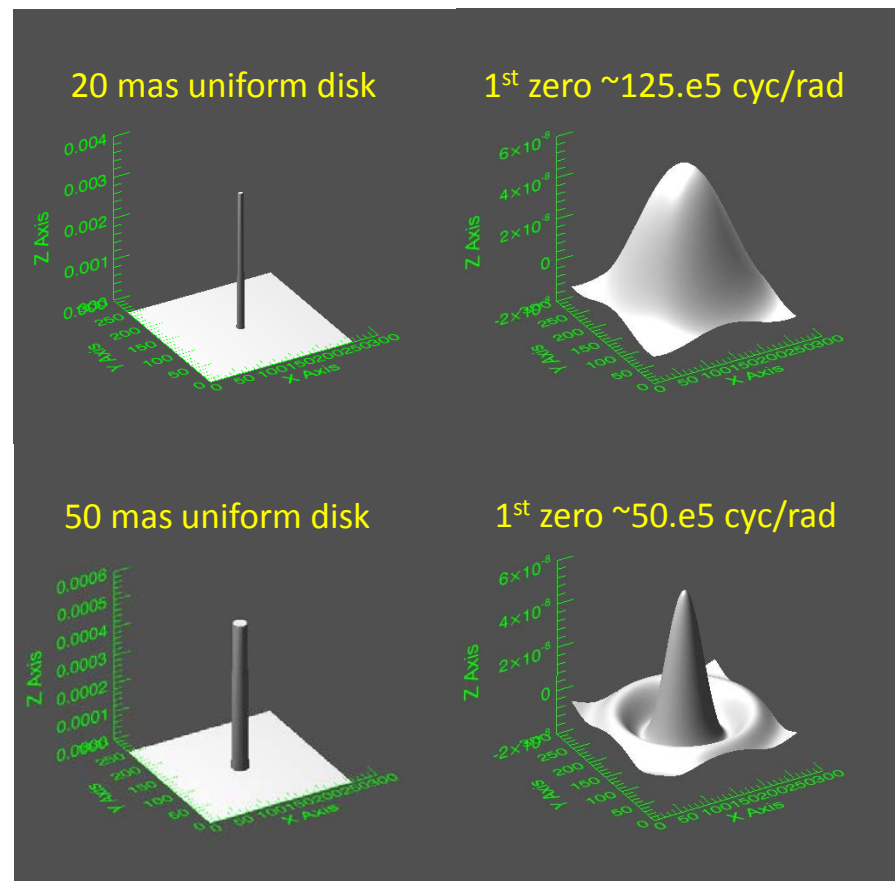
Michelson Visibility

$$V_{ij} = \frac{I_{max} - I_{min}}{I_{max} + I_{min}},$$

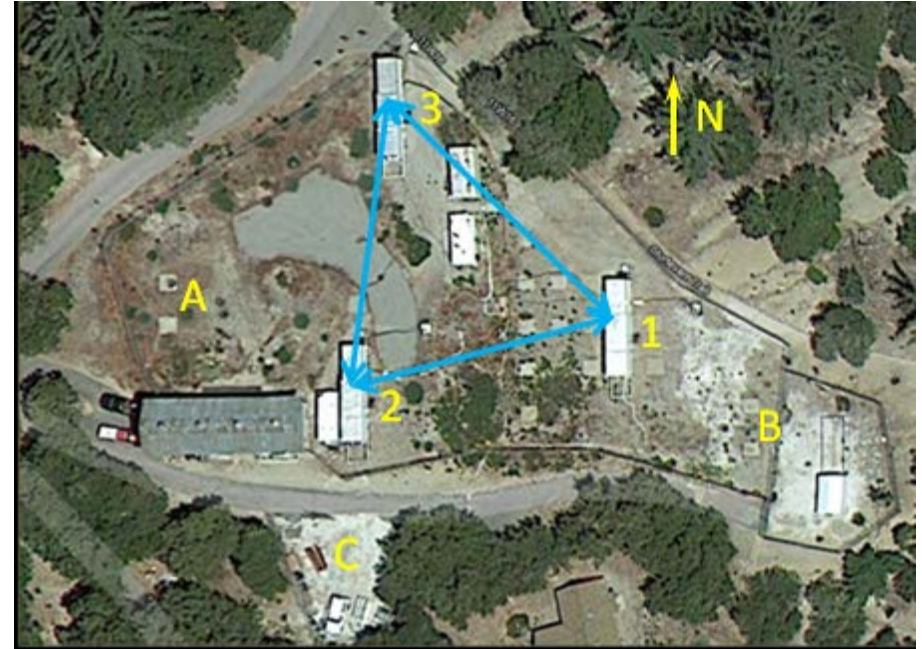
$$V_{ij}^2 = \frac{|F_{ij}|^2}{P_i P_j}.$$



Weiner, 2002

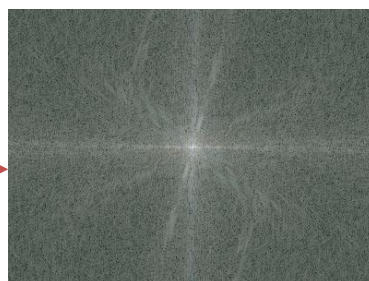
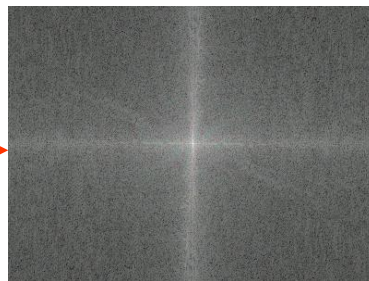


ISI array configurations and moving telescopes



ISI site. Teles. 1,2,3 are shown.
Cement pads for longest baselines EW
are A,B 85m. Longest NS baseline 3,C
~60m

How Important Is Phase?



K. Tatebe

Closure phase as a measure of asymmetry

The visibility curve is the power spectrum of the image as function of spatial freq.

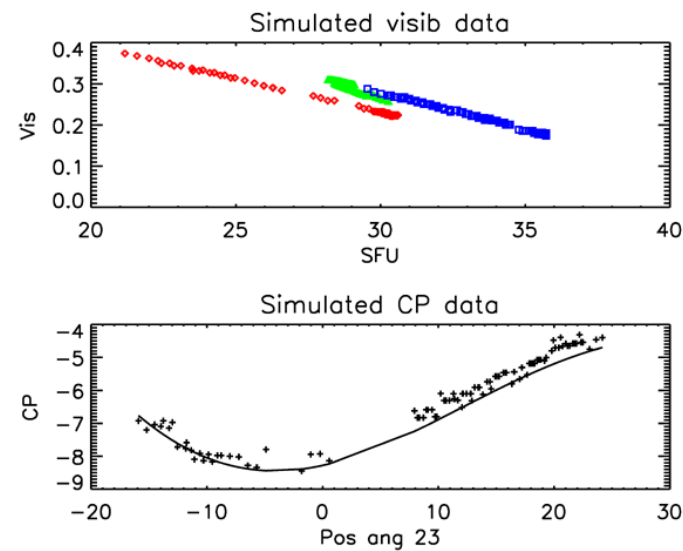
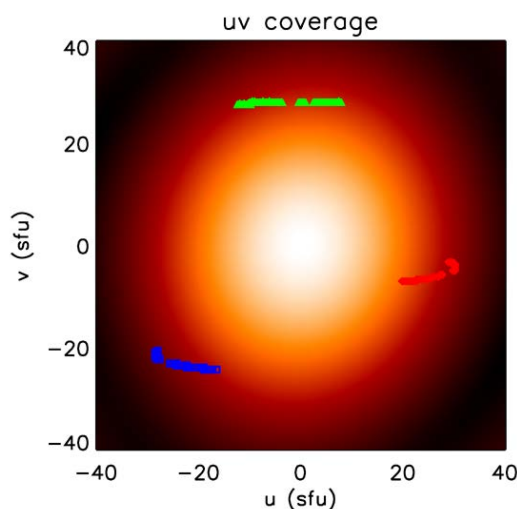
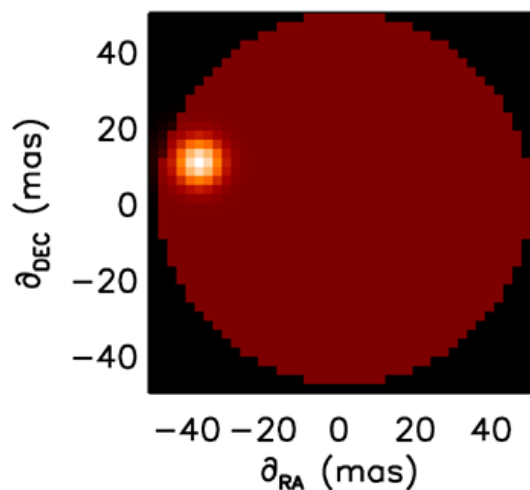
The image phase gives the positions of features in the image.

Atmospheric turbulence prevents an accurate phase measurement, but the ISI can record the *closure phase*:

$$\Phi_{CP} = \phi_{12} + \phi_{23} + \phi_{31}$$

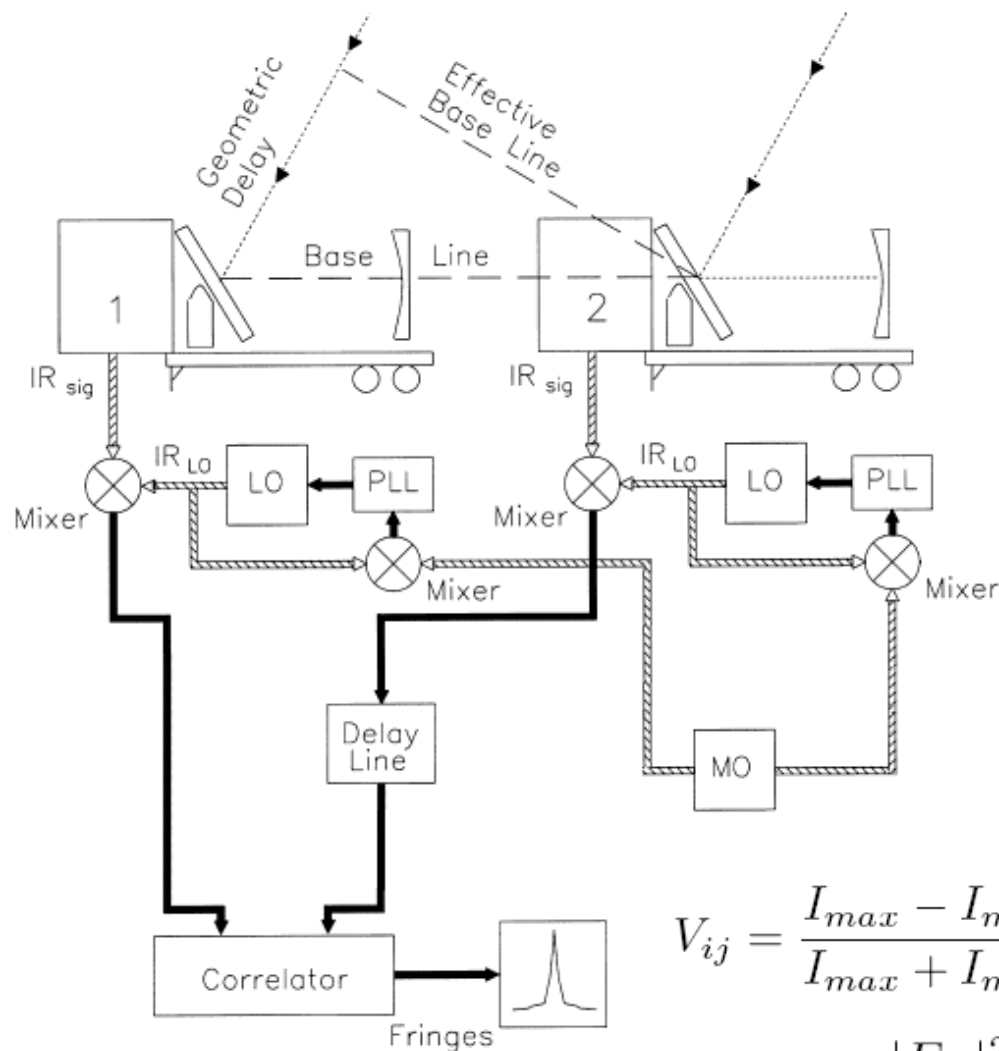
The closure phase provides vital information about stellar asymmetries.

For example, the closure phase is zero for sources which are centro-symmetric.



For samples in uv plane,
Visibility & closure phase

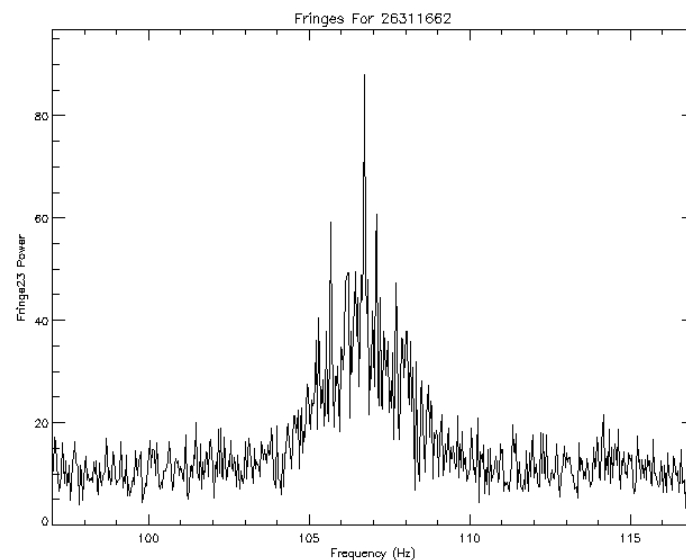
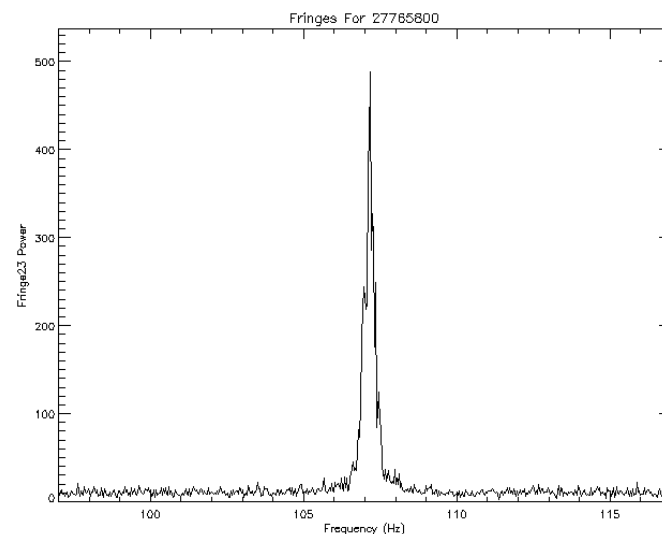
Interferometer scheme, examples of fringes



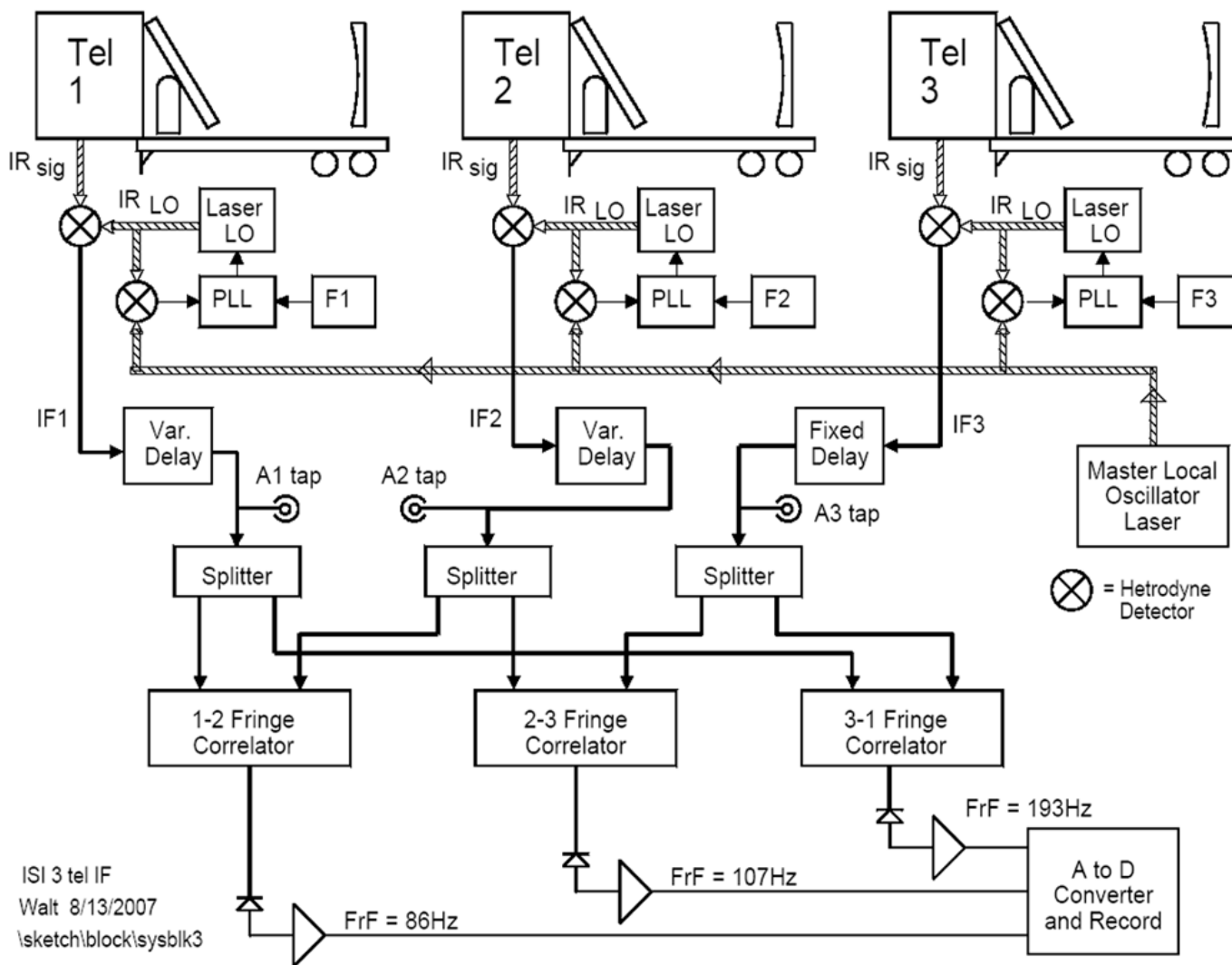
Heterodyne detection
using CO₂ lasers as
local oscillators

$$V_{ij} = \frac{I_{max} - I_{min}}{I_{max} + I_{min}},$$

$$V_{ij}^2 = \frac{|F_{ij}|^2}{P_i P_j}.$$



Current system, spectrometer taps A1,A2,A3





Heterodyne signal to noise

At detector, $E = E_{LO}\cos(w_{LO}t) + E_s\cos(w_s t) + E_0\cos(w_0 t + \delta)$

E_0 is zero-point energy fluctuations,
one photon per root bandwidth per time

Johnson & Townes 2000
Optics Comm, 179, 183

Power law detector forms product terms; including beat frequency
difference (and sum)
where $w_0 = w_s$ is the pertinent noise term

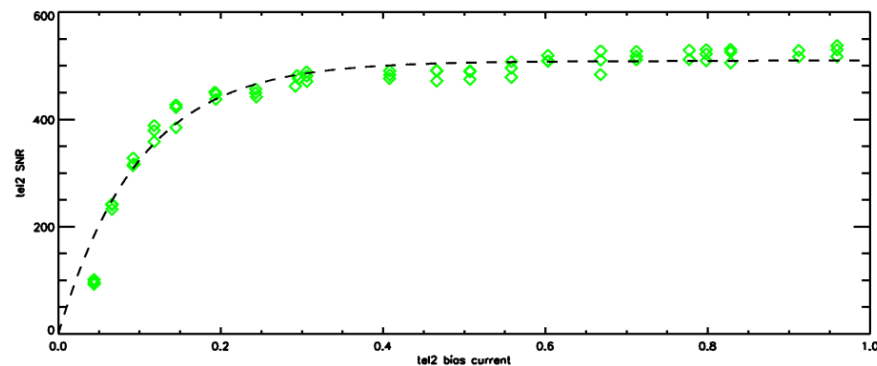
S/N heterodyne $\propto \sqrt{\Delta\nu}$ just like direct detection
however heterodyne detectors have limited b.w.

System noise temp at $11\ \mu\text{m} \sim h\nu/k = 1300\ \text{K}$
for wavelengths $> 1\ \text{cm}$, amplifier noise will dominate
for $1\ \mu\text{m}$, $h\nu/k = 14000\ \text{K}$

Multiple LO's falling on a single detector
Have increased signal and noise in same
proportion

Note that in mid-IR, at very high resolution: $R \sim 1\text{e}6$
where photon number/res element is near
read noise, Het can be superior to direct det.

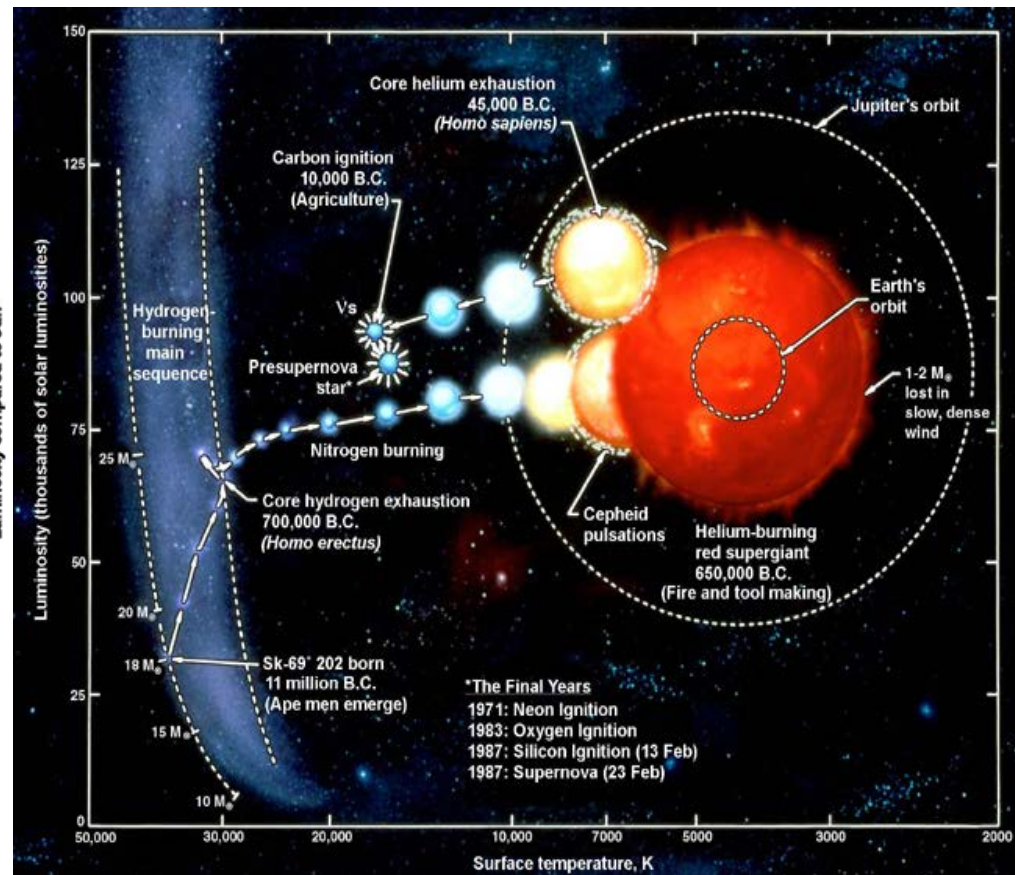
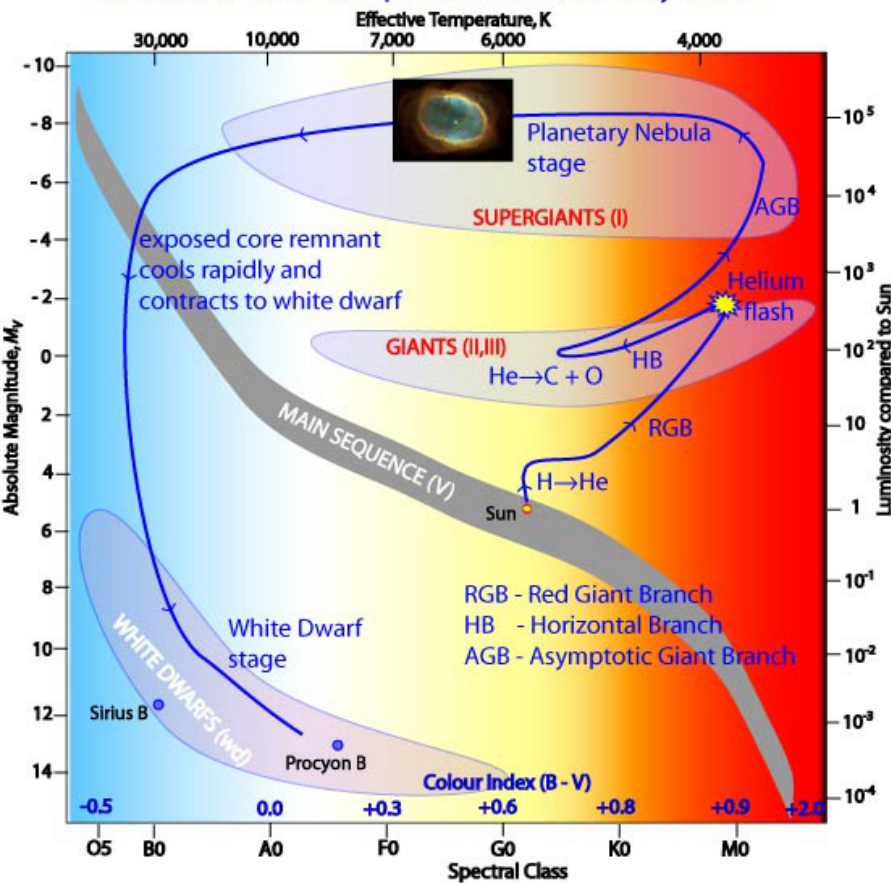
Detector test measurement
showing bandwidth limit of S/N



SNR vs. det. current \propto LO power

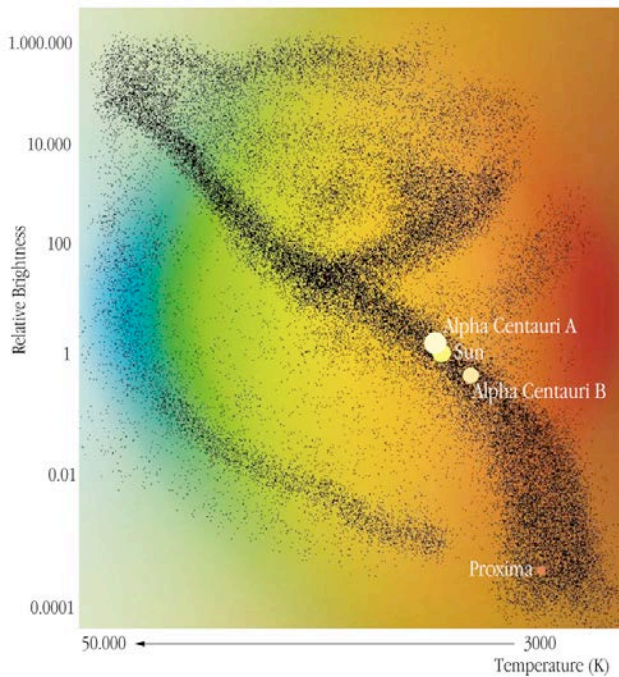
Hertzsprung-Russell Diagram & Evolutionary path of a Mira star & red giant

Sun's Post-Main Sequence Evolutionary Track

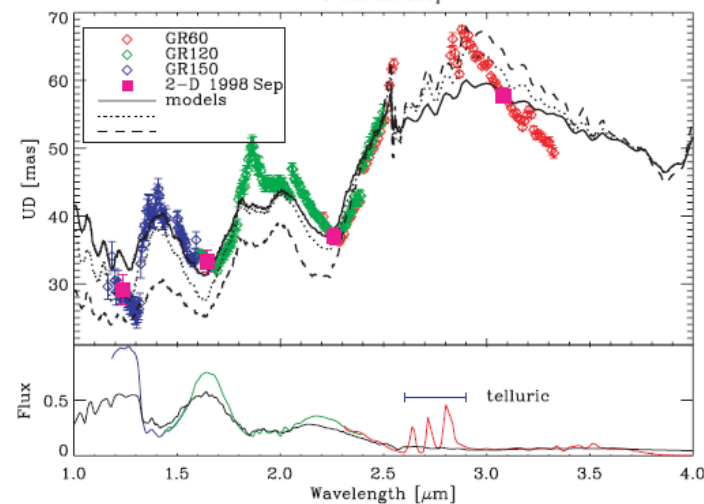


Aspects of Red Giant & Mira stars

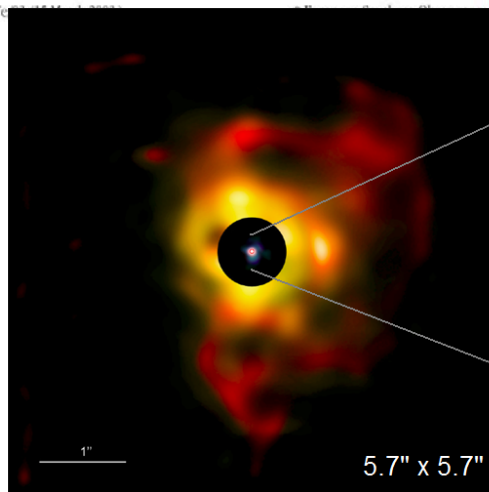
Apparent size varies with wavelength, Keck aper. mask



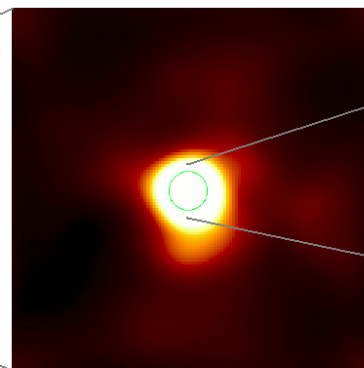
Alpha Centauri in the HR-System



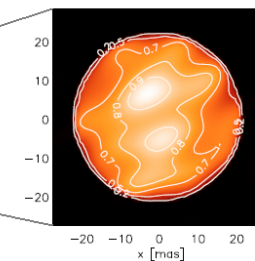
Woodruff et al.,
ApJ 691, 1328, 2009



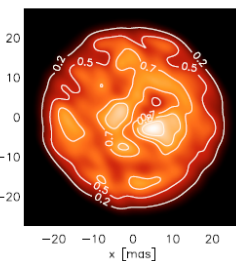
mid-IR deconvolution image
complex dust shells
(Kervella et al. 2011)



K band deconvolution image
extended atmosphere,
photosphere diam 43.7 mas
(Kervella et al. 2009)



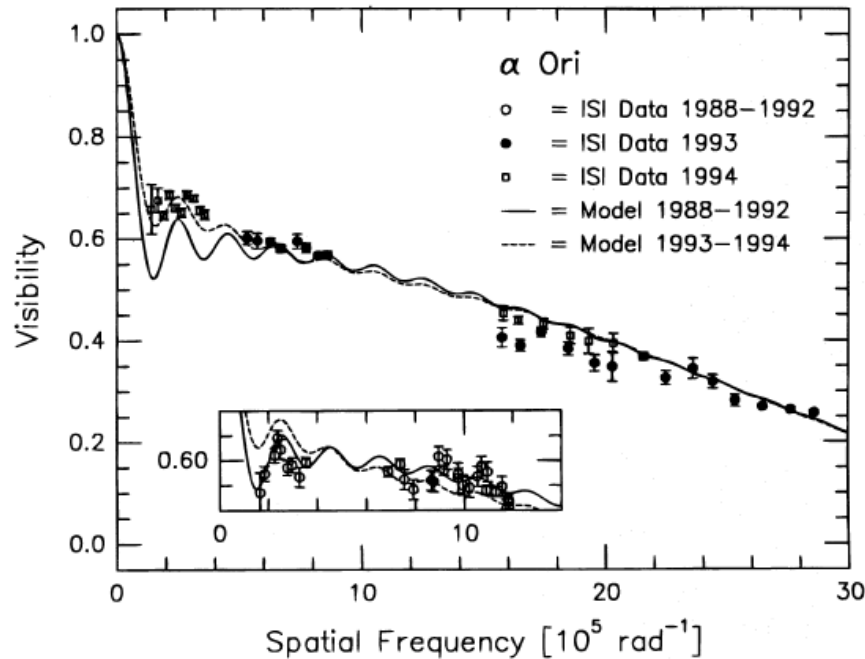
H band interferometry
with bright surface
features (Haubois et al.
2009)



numerical model image
comparison to C
(Chiavassa et al. 2010).

ISI two telescope results: Stellar variations over time

Betelgeuse visibility variations



Fringe visibility measured over various baseline distances.

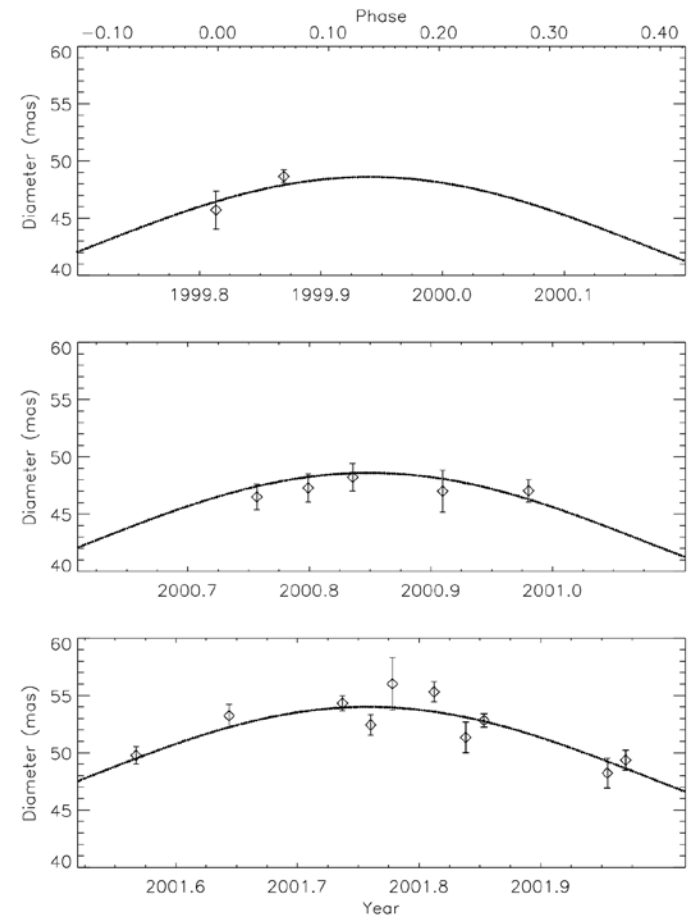
Spatial frequency in units of 10^5 cycles/radian

1 SFU = 0.5 cyc/arcsec

Two main components to the visibility curve: stellar and dust.

Bester et al. 1996

Variations in angular size of Mira over a stellar luminosity period



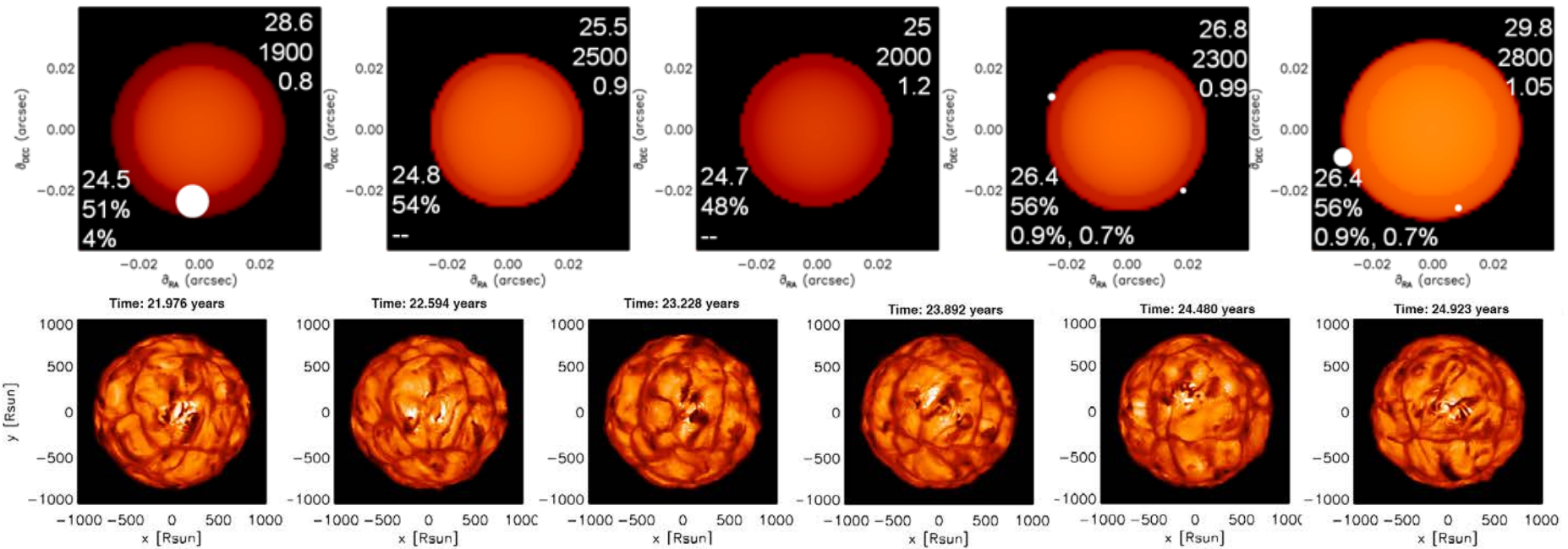
Weiner et al. 2003

The perils of daytime observing?



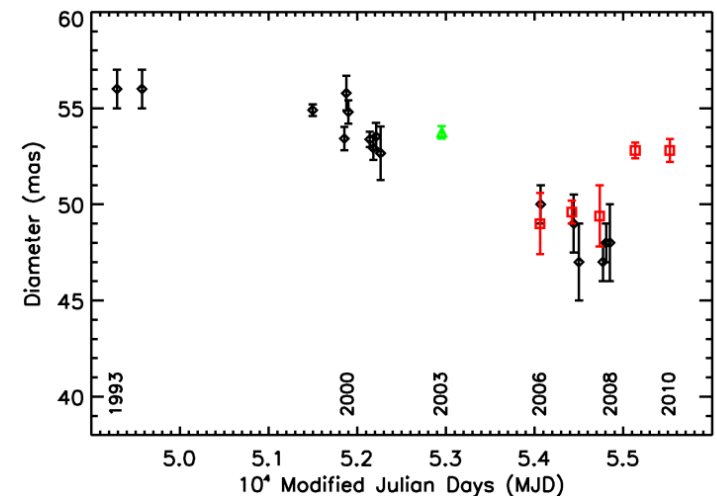
Dec 1990
Madfred Bester

Comparison of 11 μm fitted “images” to 1.8 μm theory

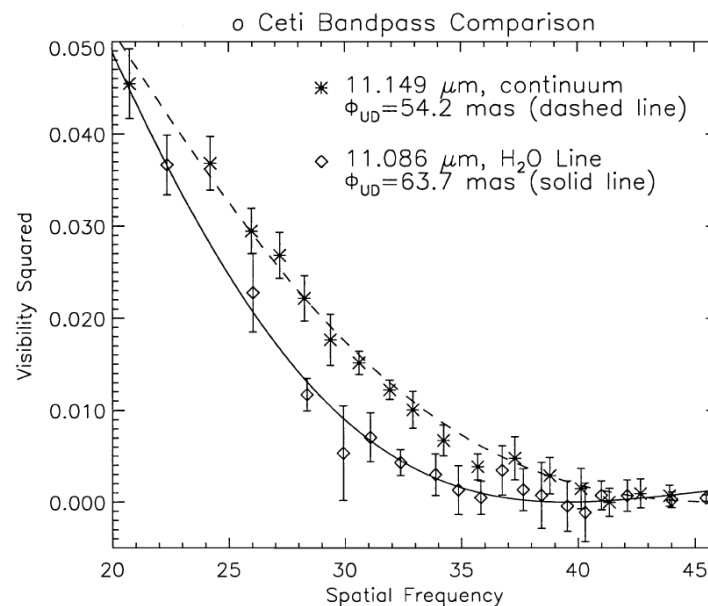
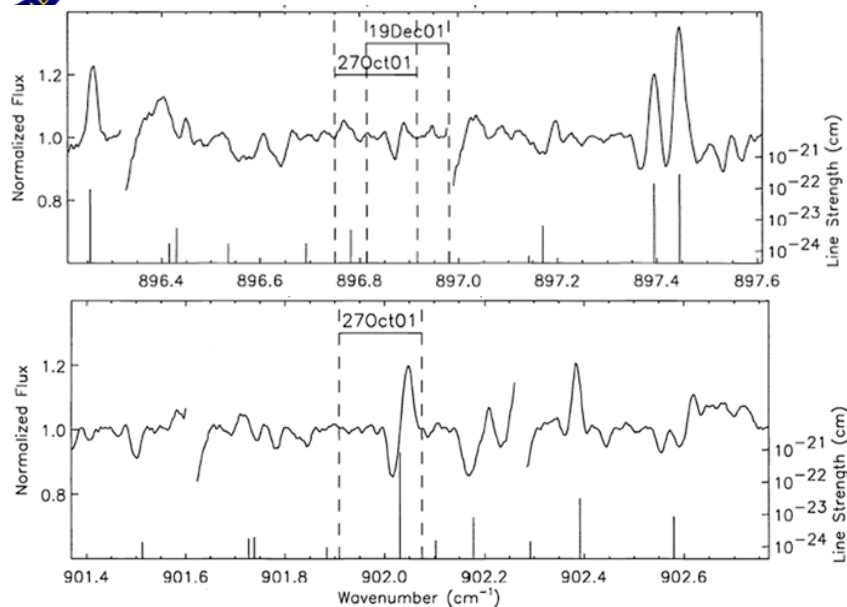


Series of theoretical images H band covering 3 years
Chiavassa et al., A&A, 506, 1351, 2009

Betelgeuse “images” and long-term monitoring of the angular size of Betelgeuse, Ravi et al. 2011



O Ceti, uniform disk fits to visibilities on-off spectral line



Weiner et al. 2003, SPIE, 4838, 172

Previous ISI

Spectroscopic-interferometry

RF analog system

VY Cma

NH₃ forms at $\sim 40R^*$

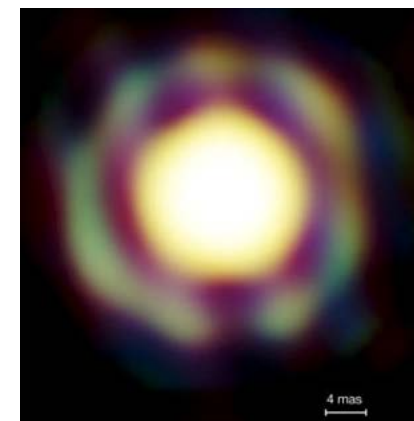
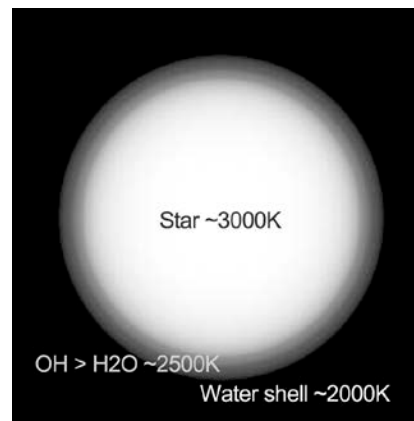
IRC +10206

NH₃ forms at $\sim 20 R^*$

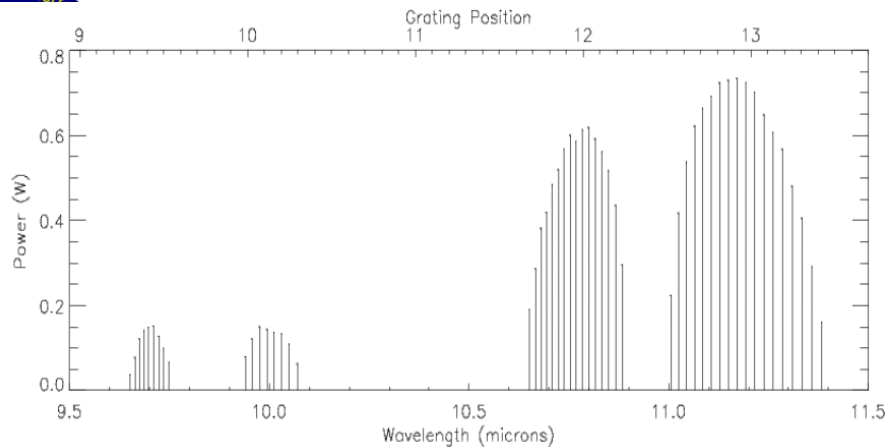
SiH₃ forming at $\sim 80R^*$

Monnier et al. 2000

ApJ, 453, 868



T Lep, VLTI, 1.4-1.9 μm ,
Le Bouquin et al. 2009 A&A L

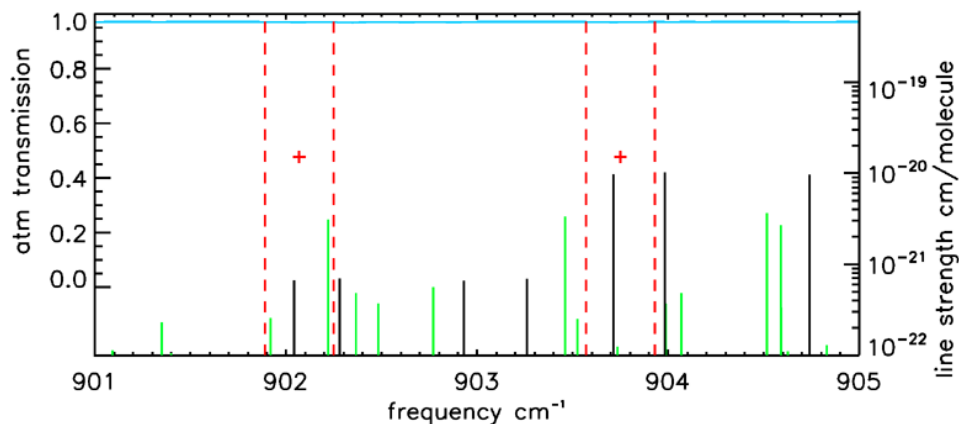
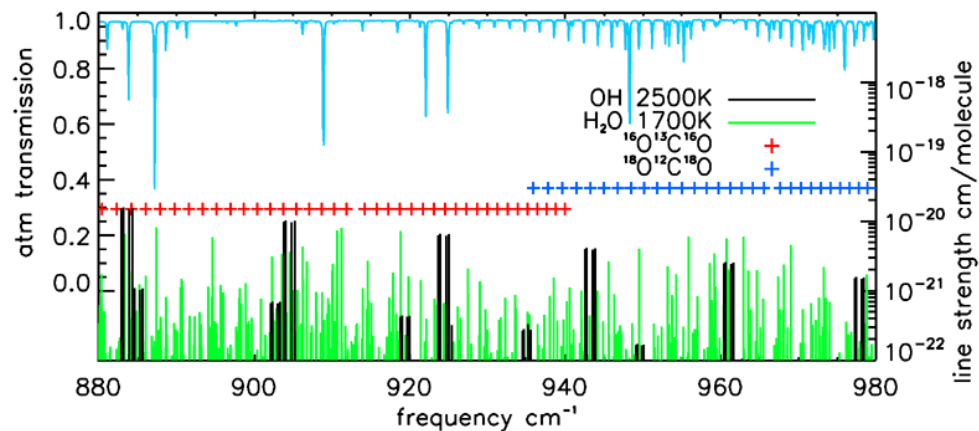


Spectral range covered,
OH & H₂O lines of interest

ISI ¹³CO₂ laser lines

Previous ISI
Spectroscopic-interferometry
RF analog system

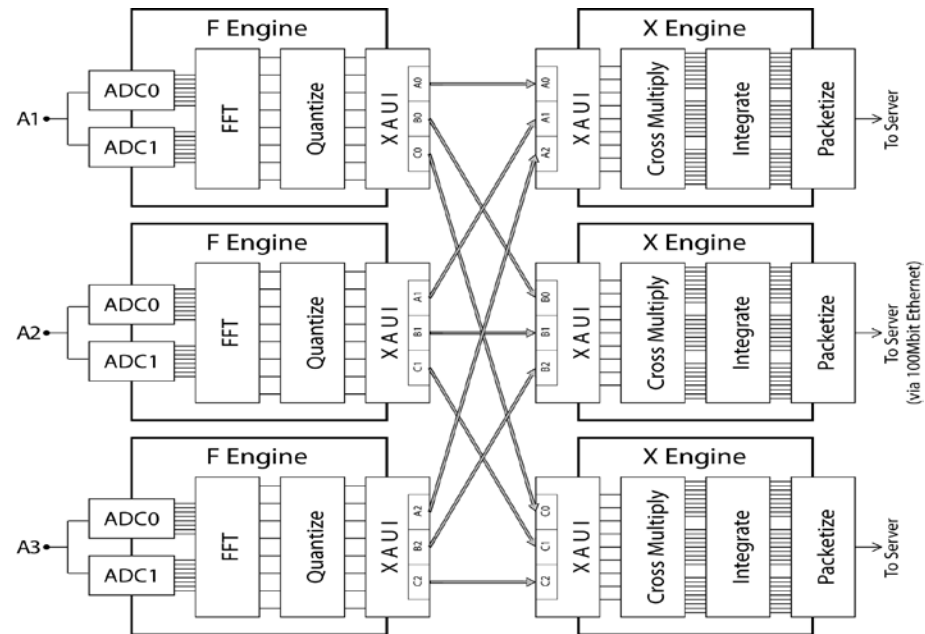
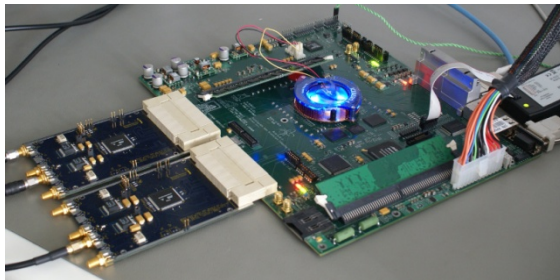
Monnier et al. 2000
ApJ, 453, 868



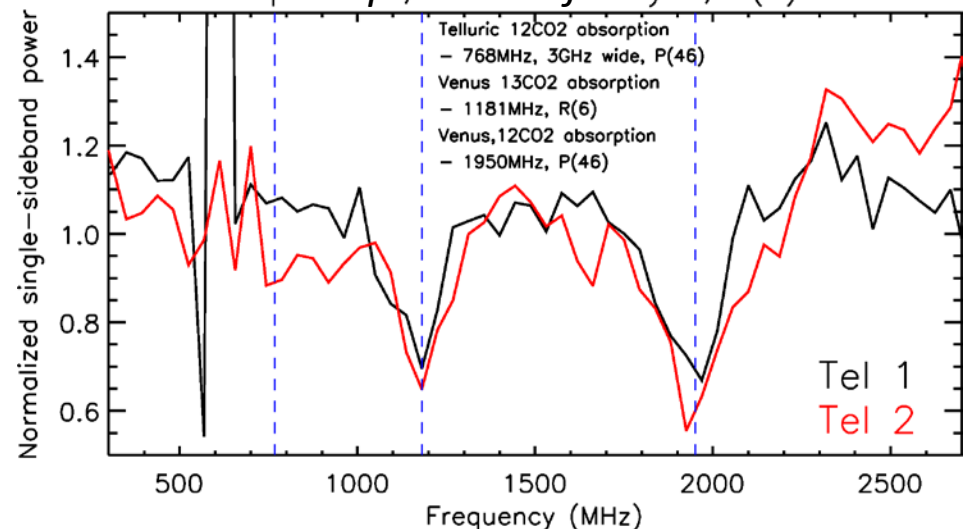
Simulation of α Ori
OH black
H₂O green
Band covered red

FPGA digital spectrometer-correlator

3 GHz BW, 64 channel
Spectral resolution of 600,000

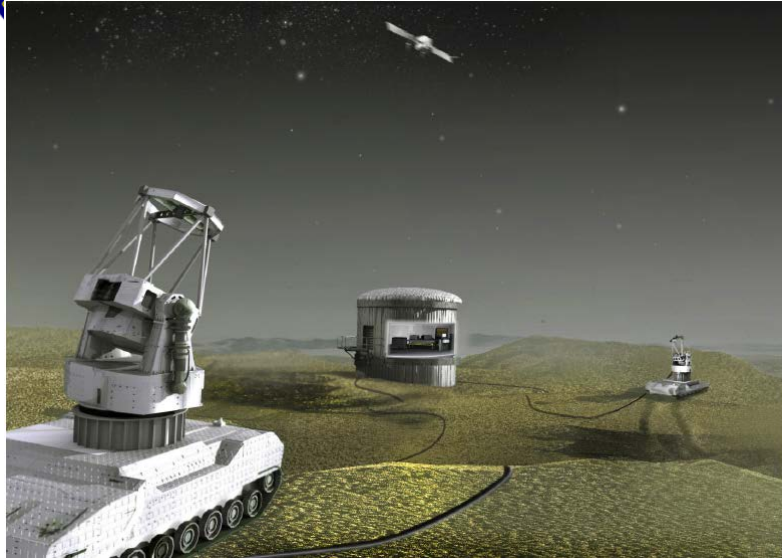


Spectrum of Venus



6 Gsamp/sec using interleaved ADCs
128 pt FFTs every 22 ns.
Data swapped between boards for cross-correlation and accumulation.
45000 spectra, every ms.
Collaboration with Mallard, Werthimer, CASPER

DARPA program to image geo-synchronous satellites



Interferometry of geo satellites

10 cm resolution @ 36000 km

~ 3 nrad ~ 0.6 mas, V band magnitude = 11

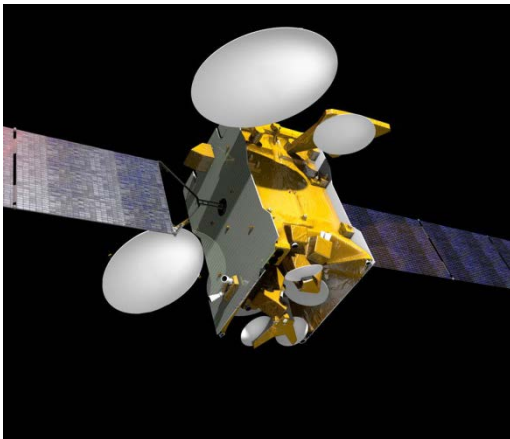
Many samples in UV plane to form images

Telescopes w/ /AO

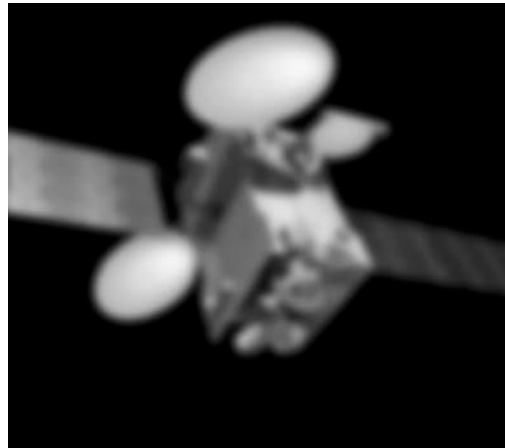
linked with optical fibers

Move baselines in 5 min

Conduct meas. at Starfire in NM



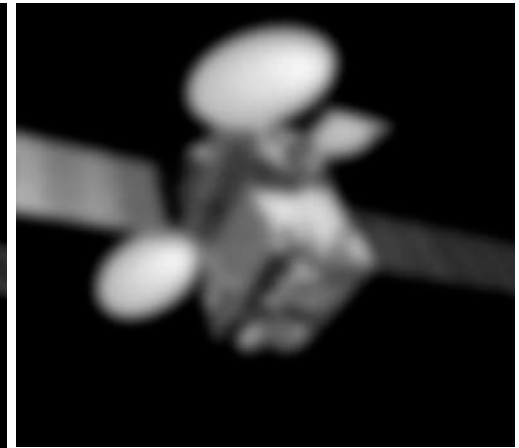
Sat image



~ 10 cm resolution

1 μ m wavelength

360 m baselines



~ 40 cm resolution

1 μ m / 100 m baselines

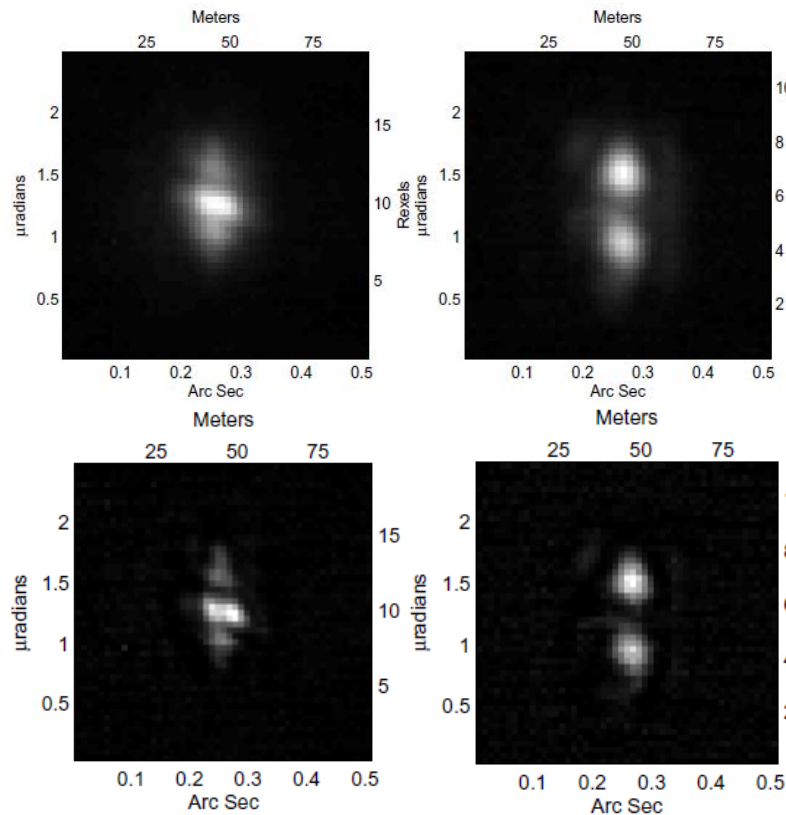
10 μ m / 1km

Status of Program?

Similar to Planet Formation Imager?

10 μ m / 7 km

Data from geo-satellites, 10 μm is a poor region



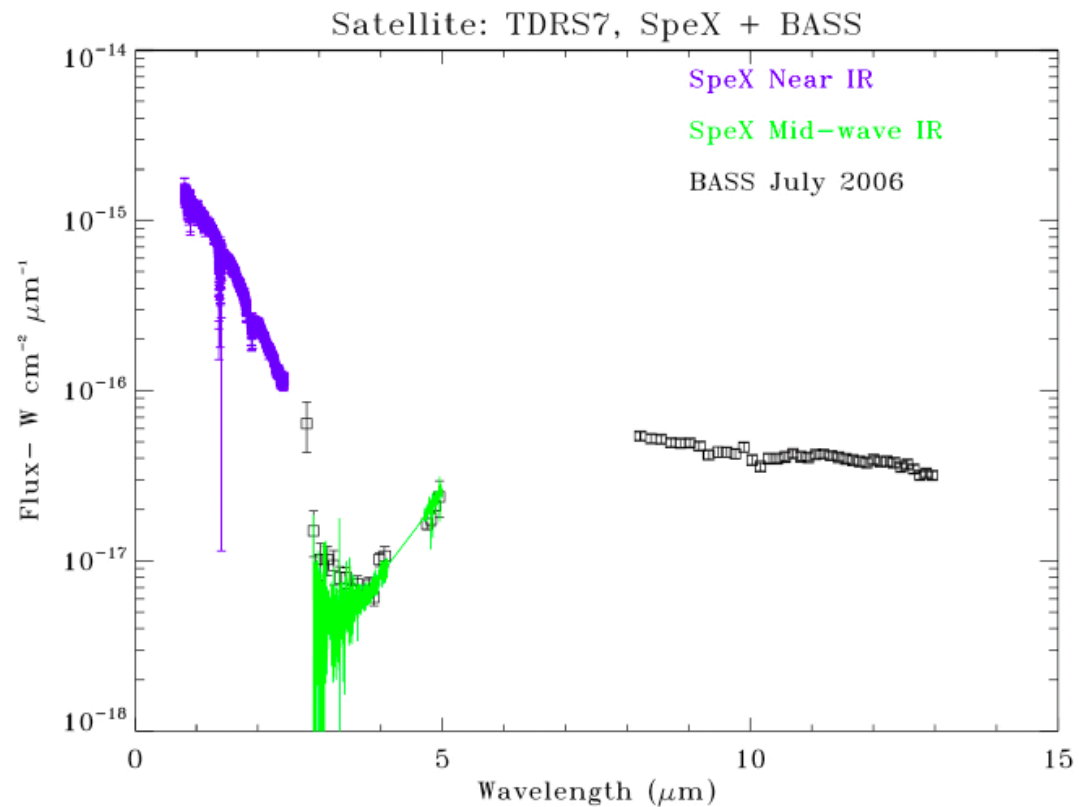
Data from Keck AO.

Drummond, Rast 2010

Left: 1.25 μm , Right: 2.17 μm

Below deconvolved images

dtic.mil/get-tr-doc/pdf?AD=ADA531722



Data from IRTF

Skinner, et al., IR spectro-photometric observations of Geosynchronous satellites, in: Proceedings of the AMOS Technical Conference, September 2007, Maui, HI, 2007.

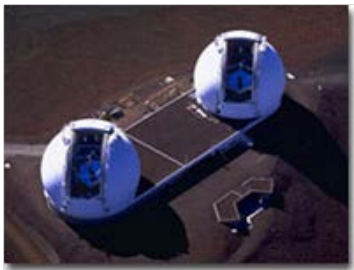
Other optical-IR interferometers



NPOI
6x12 cm
Augment w/
Keck outrig



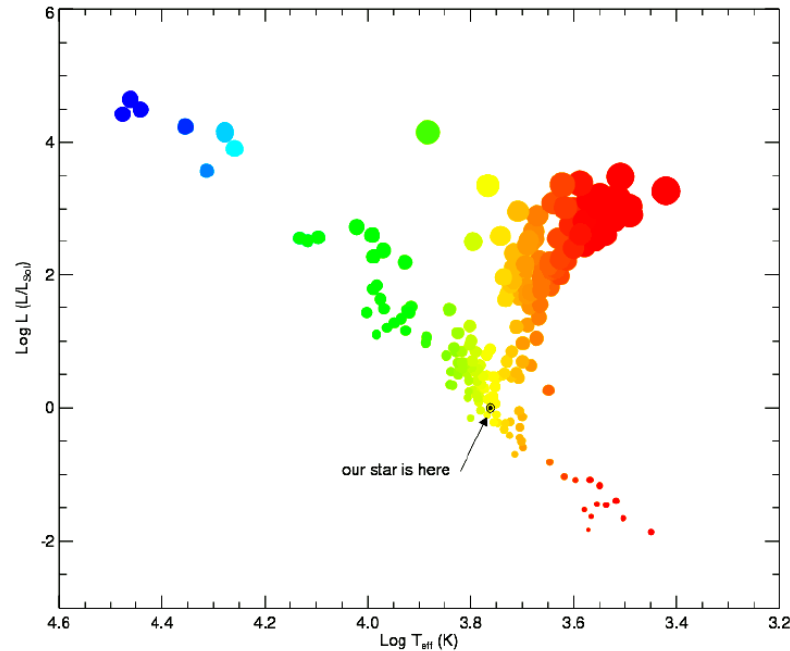
CHARA
6x1m



Keck
2x10m



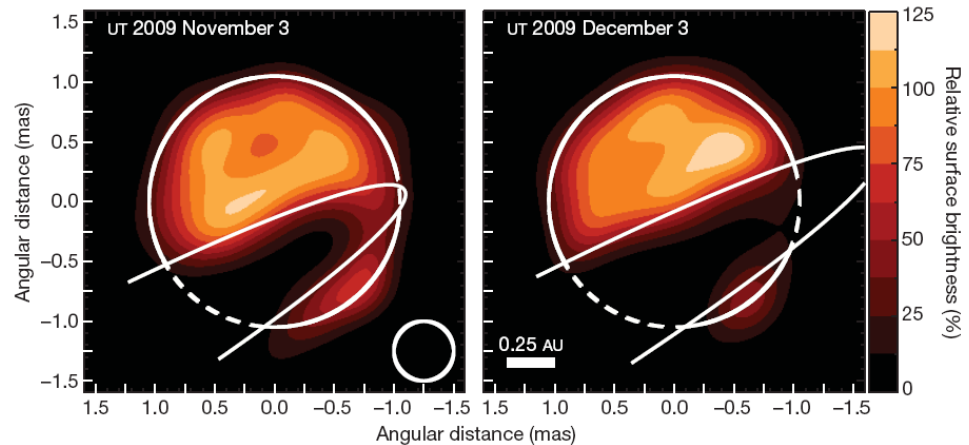
Magdalena Ridge
under const.



HR diagram of 250
measured stellar
diameters

Physics Today,
June 09

Boyajian, CHARA



Kloppenborg et al. Nature, 464, 870, 2010

Epsilon Aurigae and eclipsing binary (25 yr. period)
F star, with orbiting B star enshrouded by a disk

Also LBT, VLT--Gravity



Three telescope array, ~36 m baselines

Sean Lockwood/Walt Fitelson



Biswaroop Mukerjee

Group photo, illuminated by moonlight



Dave Hale

Three telescope linear array, 4,8,12 m baselines



Backup slides



SETI Studies



No. 4772

April 15, 1961

NATURE

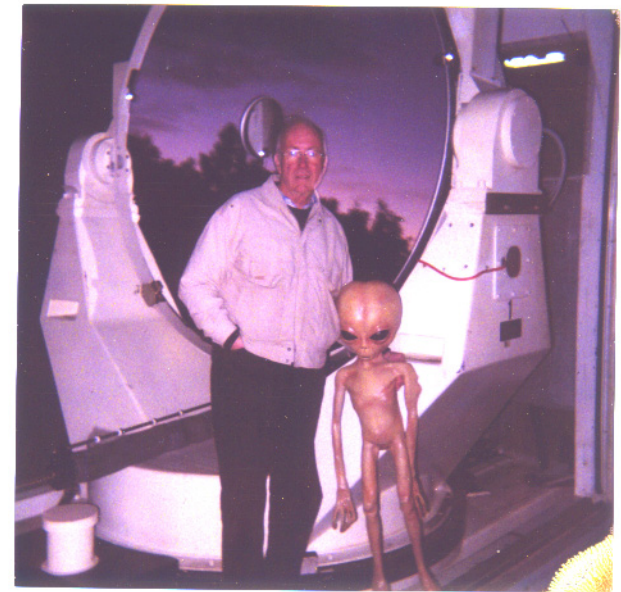
205

INTERSTELLAR AND INTERPLANETARY COMMUNICATION BY OPTICAL MASERS

By DR. R. N. SCHWARTZ and PROF. C. H. TOWNES*

Institute for Defense Analyses, Washington, D.C.

Thus, it appears that if one postulates the existence of an optical maser system beamed towards us of the characteristics of system (a) at a distance of the order of 10 light-years, it is within the state-of-the-art for us to detect it.

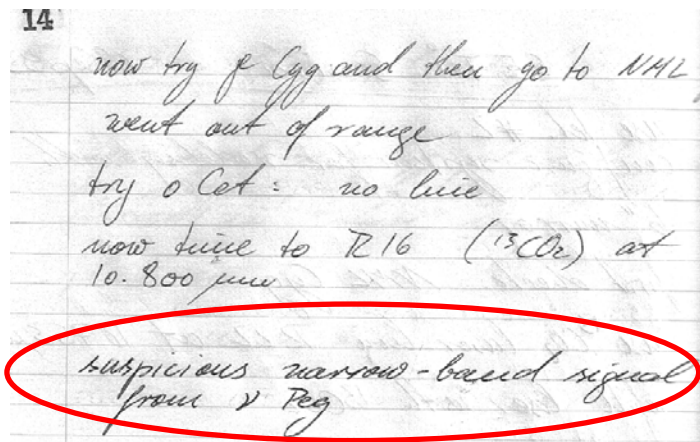


???

Theoretical and experimental work continued by Betz

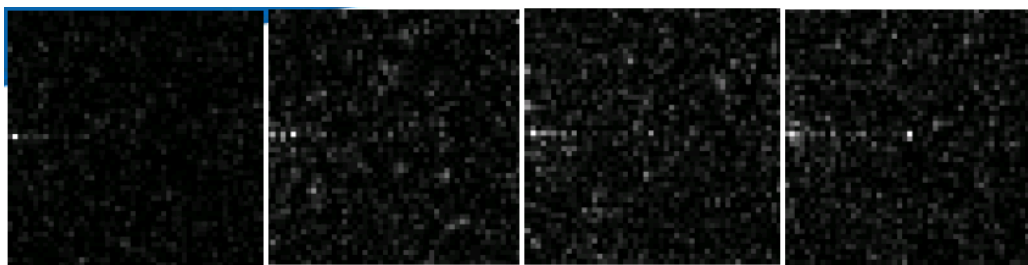
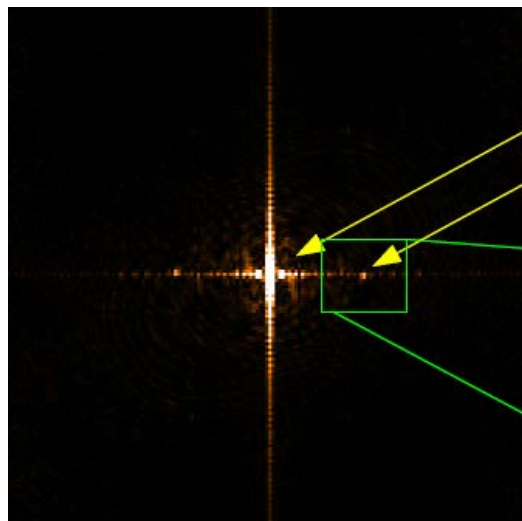
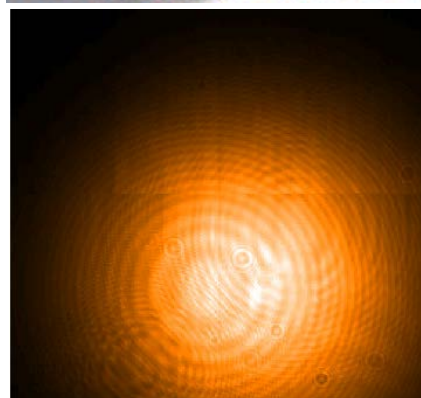
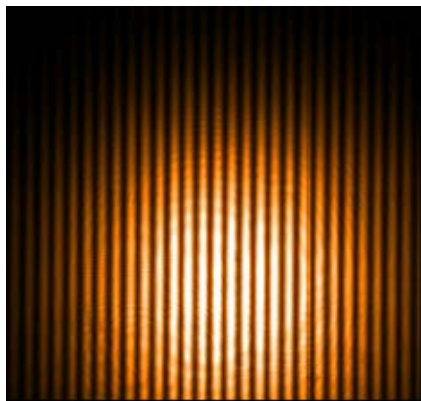
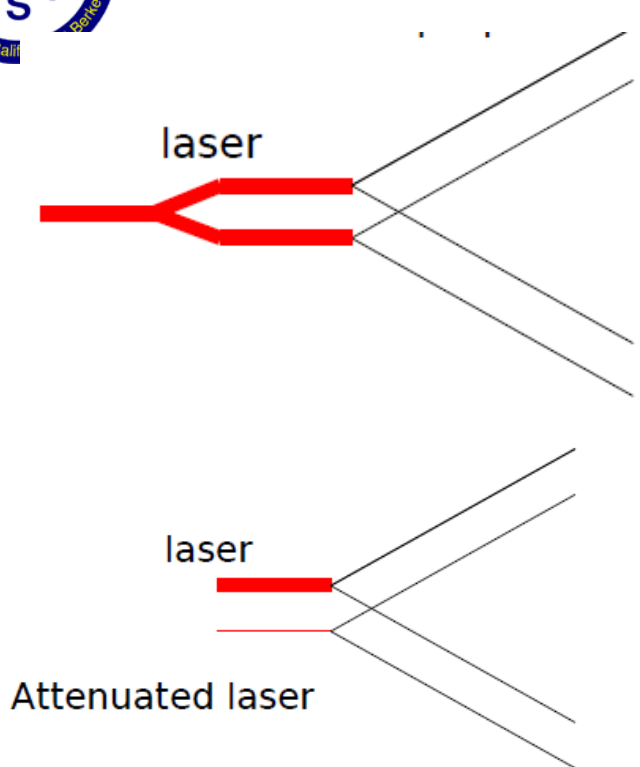


Participating in ongoing Panchromatic search,
support from Templeton Foundation.



Bester notebook sep 1993

Photonic Heterodyne?



0ph

1ph

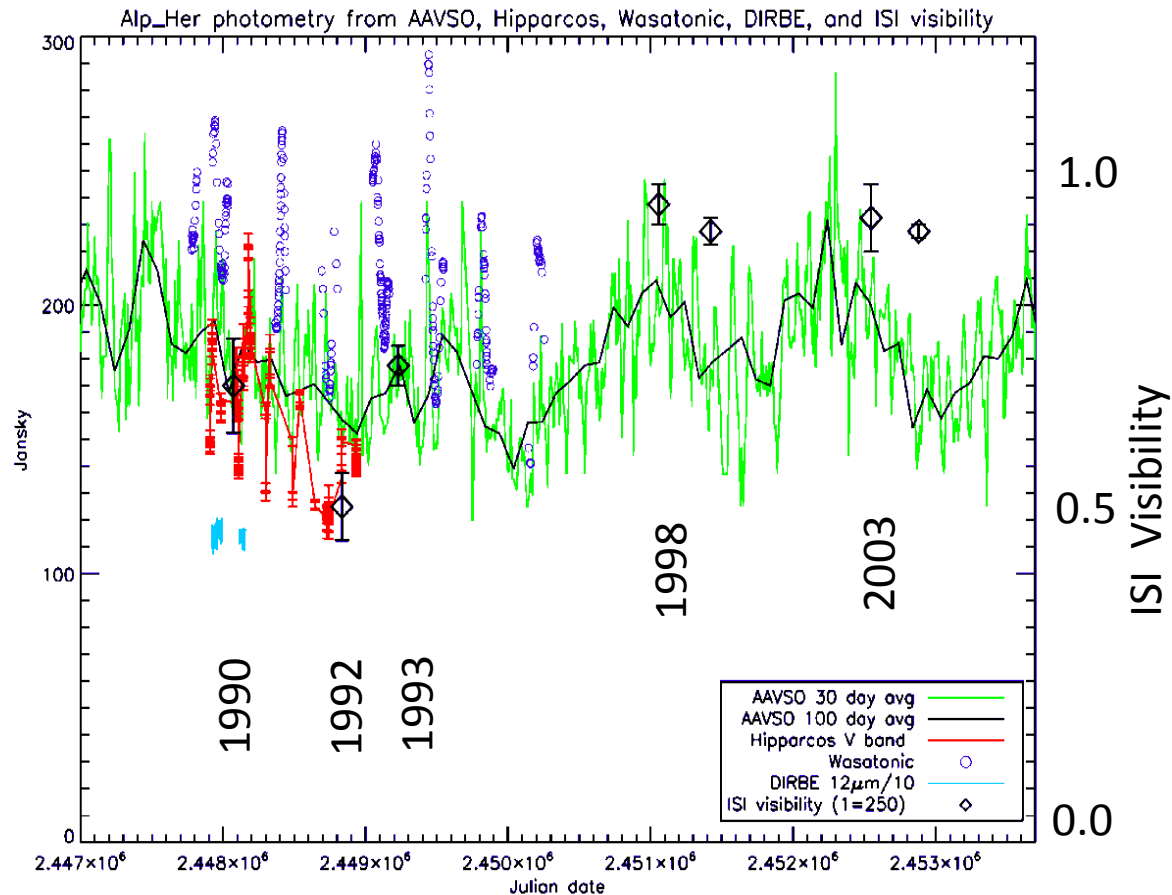
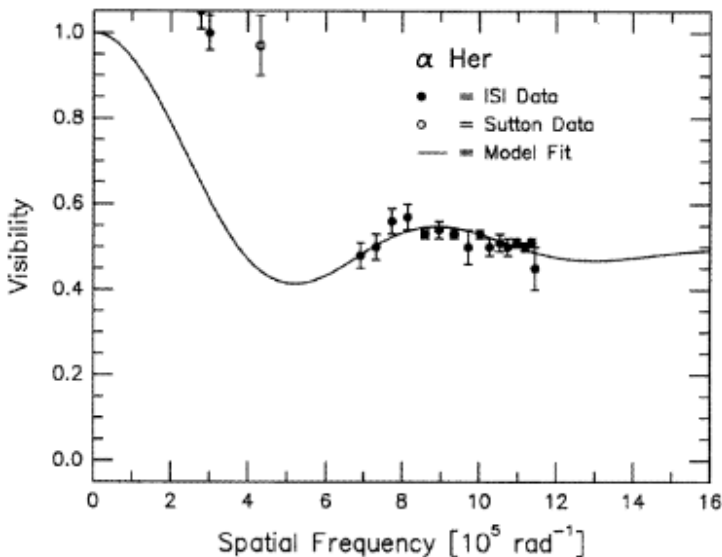
2ph

3ph

Laser & fast camera

Ettiene Le Coarer, Renewing Heterodyne, OHP 2013

Long term studies: variations of α Her

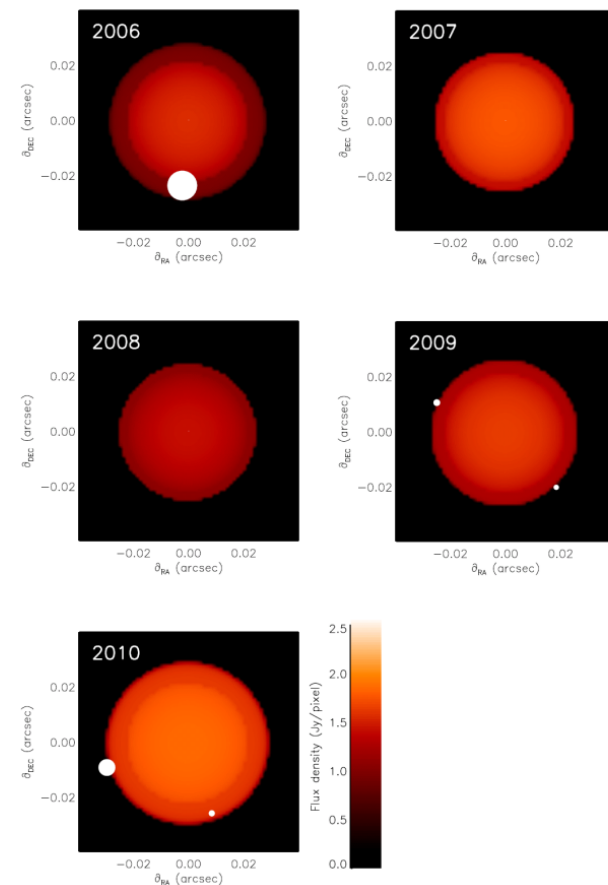
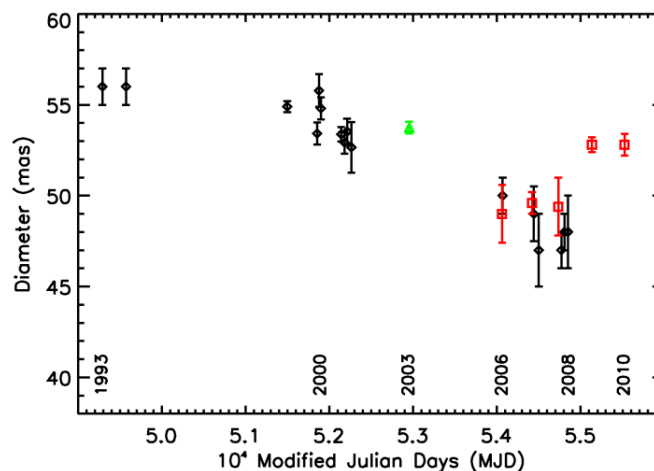
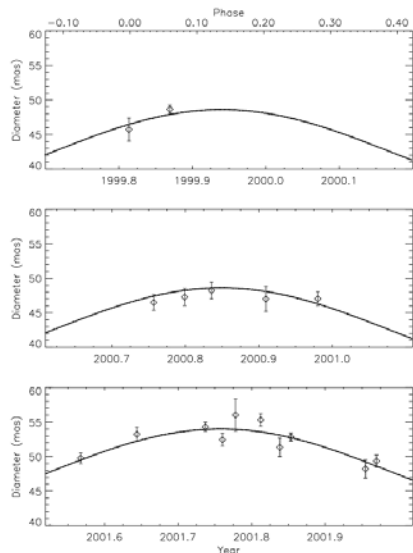


Tatebe et al. "Observation of a Burst of High-Velocity Dust from α Herculis,"
2007, ApJ, 658, 103. From 92 to 93, about 75 km/sec



Infrared spatial interferometer (ISI)

Combines High Spectral resolution, high angular resolution and new techniques



Variations in angular size of Mira compared to luminosity phase
Weiner 2000

Long-term monitoring of the angular size of Betelgeuse
Ravi 2011

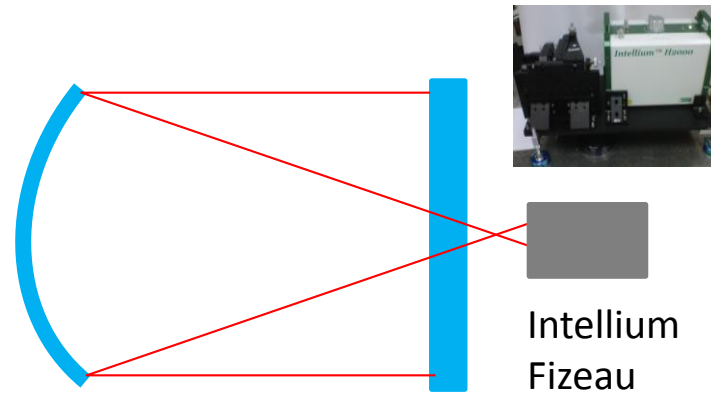
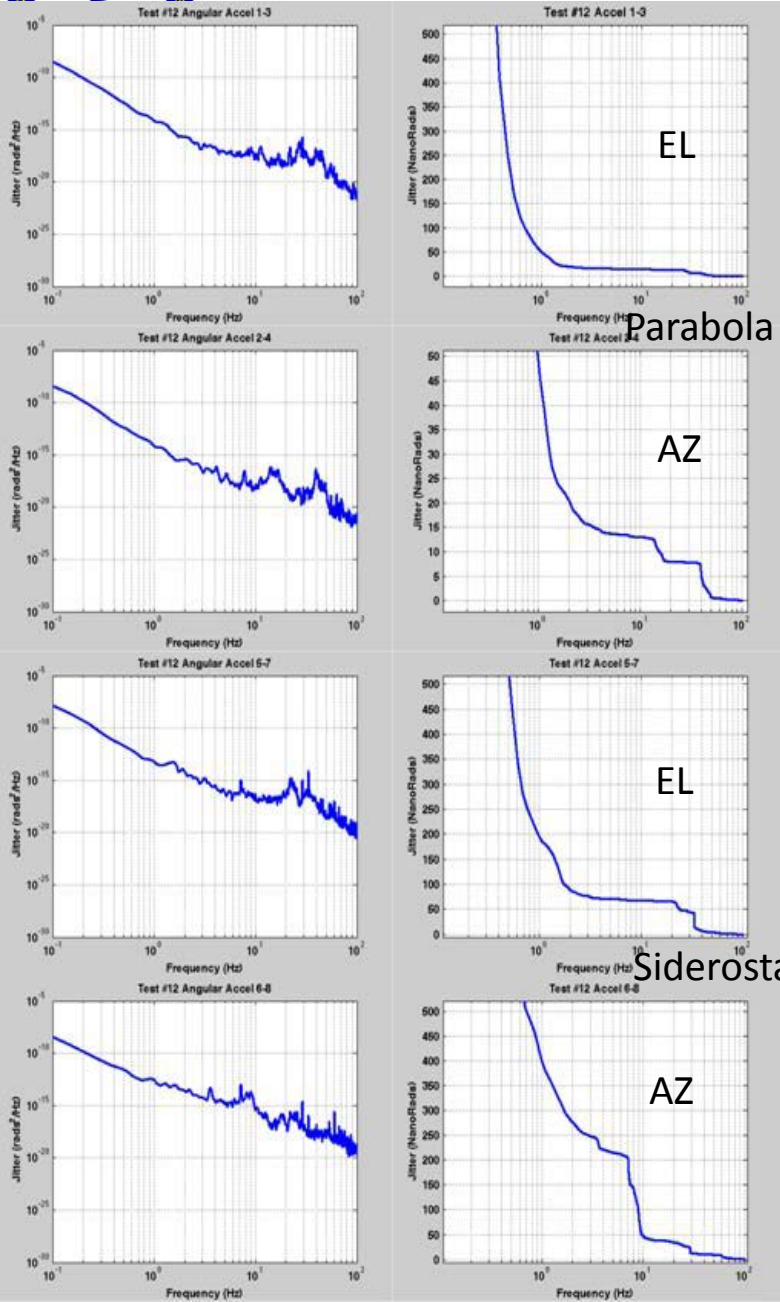
Measurements of dust shells surrounding red giant stars and their surprisingly rapid changes with time. Danchi 1994, Bester 1996, Tatebe 2007

Measurements that NH₃ and SiH₄ form at 20-40 and 80 stellar radii from stars, respectively. Monnier 2003

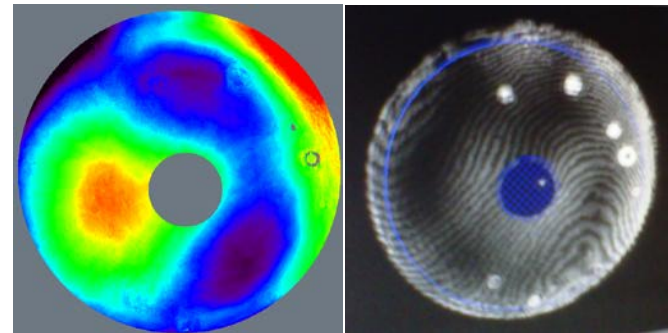
Measurements of dust shell asymmetries using 3 telescopes and phase closure. Tatebe 2006, Chandler 2007

Variations in stellar shape and "hot-spots" of Betelgeuse
Ravi 2011

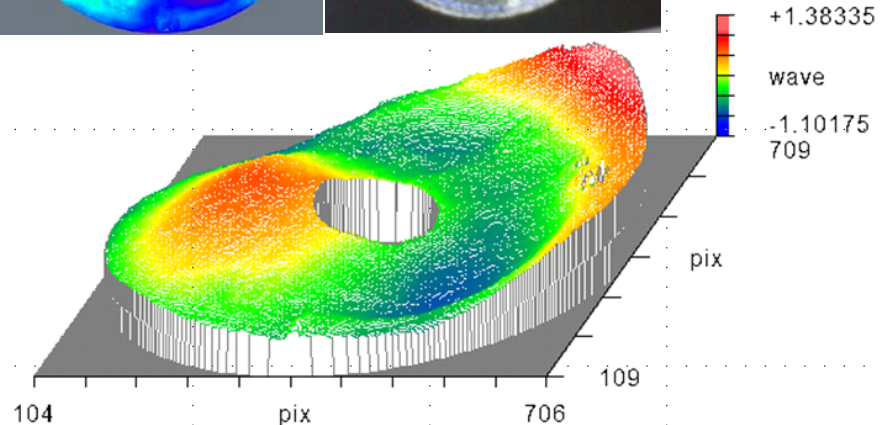
ISI Vibration tests/Optical wavefront tests



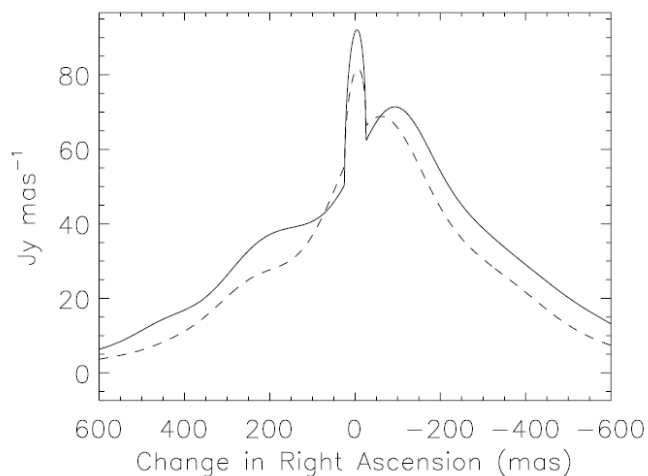
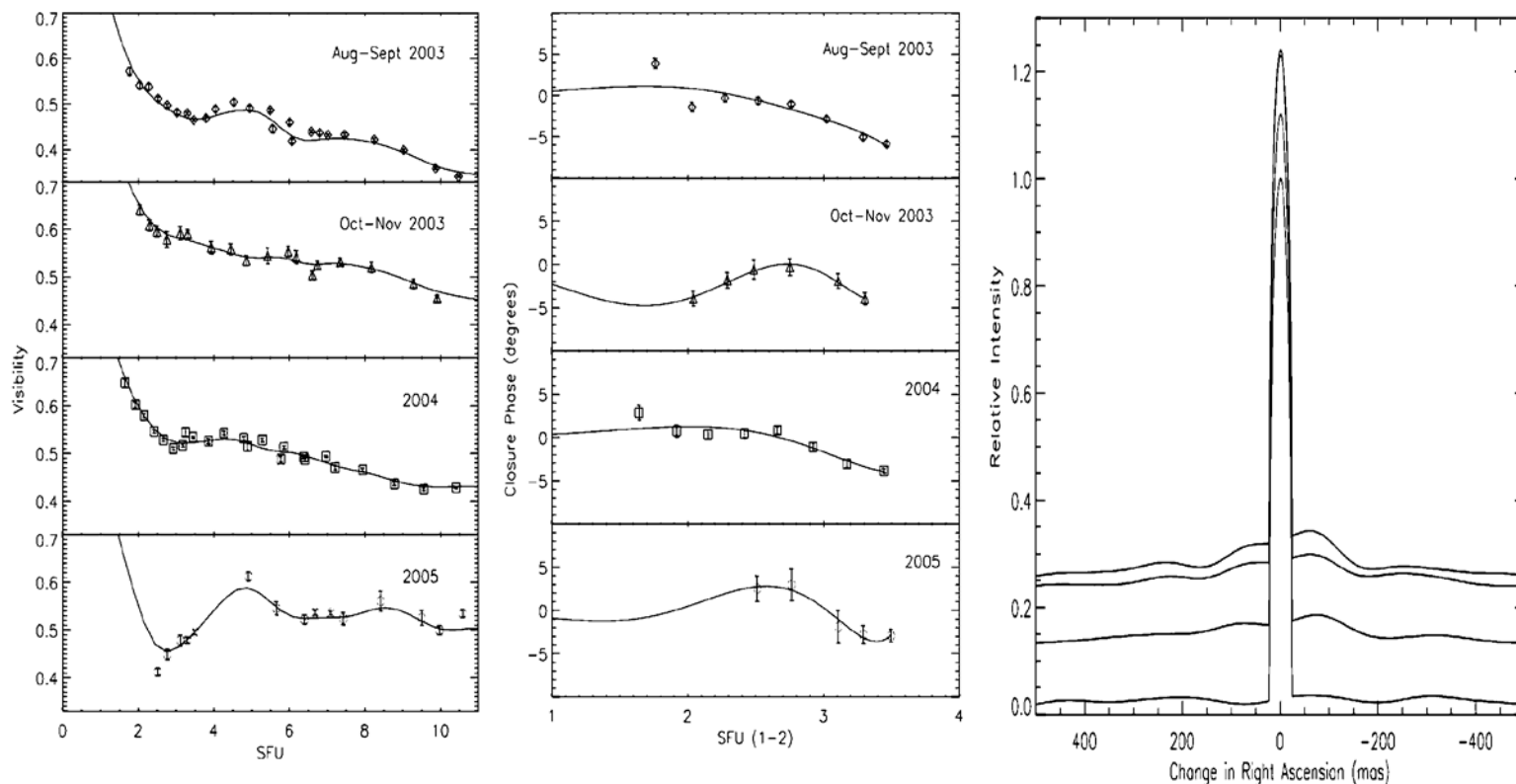
Double pass meas of ISI mirrors



PV	2.485	wave
Rms	0.382	wave
Power	0.023	wave
Aberration	wave	angle
Tilt	1.537	-162
Focus	-0.794	
Astigmatism	1.147	35
Coma	2.315	18
Spherical	0.756	



Using Phase Closure: Evolution of dust surrounding stars



Asymmetry of dust
IRC+10216
2004 (solid)
2006 (dashed)

Chandler et al., ApJ 657,
1042, 2007

In descending order:
Aug-Sep 2003
Oct-Nov 2003
2004
2005

Chandler et al., ApJ,
670,1347, 2007